

Spectroscopic and Quantum Computational Investigation of 3-Cyano chromone

Parthasarathi. A¹, Jayasheela. K², Prabhu. T³, Karthikeyan. S⁴, Periandy. S⁵

Abstract - In the present study, Molecular docking, Reduced density gradient analysis, Electron Localization function (ELF) analysis were carried out. FT-IR, FT-Raman, NMR and UV spectra of 3-cynochromone are recorded at the appropriate ranges. The fundamental vibrational frequencies are tabulated and assigned. Quantum computations were carried out using B3LYP method with cc-pVDZ basis sets and the corresponding results are compared with the experimental values. The change in the chemical environment of the compound is studied using NMR chemical shift values. The ¹³C NMR and ¹H NMR chemical shifts were calculated using the gauge-independent atomic orbital (GIAO) method, with the B3LYP functional and the cc-pVDZ basis set and their spectra is compared with the experimental spectra. A study on the electronic and optical properties; absorption wavelengths, excitation energy, density of state, dipole moment and frontier molecular orbital energies were also performed using DFT methods and UV-Vis spectrum. The calculated HOMO and LUMO are displayed with energy gap, which show the occurrence of charge transfer within the molecule. NLO properties are related to polarizability, dipole moment and hyperpolarizability, and thermodynamically parameters are also discussed.

Keywords - Molecular docking, RDG, ELF (2D & 3D), NMR, vibrational and cc-pVDZ basis set.

I. INTRODUCTION

Cyano derivatives are ubiquitous in nature. The cyano group is considered one of the most abundant functional groups on earth, second only to the amino group [1].

It is also present in significant amounts in dense interstellar clouds [2] and comet. Roughly 2000 plants produce cyano compounds, some of them being cyanogenic glycosides [3]. In organic synthesis, cyano groups play a very special role. They are not only

active groups in pesticides, medicines, and dyes, but also important radicals of aldehydes, amines, amidines, thiophenes, triazoles, tetrazoles, and carboxylic acids [4]. Moreover, cyano substitution plays a specific role in molecular modification techniques because the CN group can affect p-conjugation, leading to significant changes in the strength of adjacent bonds [5]. As the cyano group has specific electric properties and structural features, it is always used in the synthesis of new compounds. As a small substituent with strong electron-withdrawing properties, the CN group enables the establishment of intermolecular contact between molecules in the solid state [6]. The possible crucial role of HCN and polycyano compounds in prebiotic synthesis and chemical evolution, for example, has interested researchers for decades. The universality of the CN group is reflected in polycyano compounds that act as dyes or organic metals. Polycyano anions are important ingredients of materials exhibiting very strong electrical conductivity. It is quite possible that polycyano derivatives of organic molecules will play a significant role in superacid–superbase chemistry in the future [7]. Chromone is a derivative of benzopyran with a substituted keto group on the pyrone ring. Chromone is oxygen-containing heterocyclic compounds. Chromone are the subject of increasing interest due to a wide use of these heterocyclic compounds as structural building blocks for the design of various promising pharmacological agents and components for super-high capacity optical archive storage systems. Although the chromone core does not contain a nitrogen atom, chromone natural products are classified as alkaloids because nitrogenous moieties are usually attached to them [8]. In the FDA Orange Book, the chromone core is one of the top 100 most used ring systems for small molecule drugs listed [9].

Chromone exhibit important pharmacological activities, such as anti-inflammatory and anticancer due to their well-recognized antioxidant properties [10]. These compounds show the variety of pharmacological activities and the change in their structure offer a high degree of diversity that has been found useful for the search for novel therapeutic agents. It is common and integral constituent of a variety of medicinal agents [11]. Chromone-based drugs exhibit anticancer, anti-HIV, antioxidant, anti-inflammatory, analgesic, antimicrobial, antimalarial, anti-diabetic, anticonvulsant, antiplatelet, gastroprotective, antihistaminic, antihypertensive, and insecticidal activity [9-11]. Several other significant studies have also been reported along the years on the medicinal application of simple Chromone, such as

Parthasarathi. A, Department of physics, A.V.C. College, Mayiladuthurai, Tamil nadu-609 305.

Jayasheela. K, Department of physics, Kanchi mamunivar center for post graduate studies, lawspet, Pondicherry-605 008.

Parbhu. T, Department of physics, A.V.C. College, Mayiladuthurai, Tamil nadu-609 305.

Karthikeyan. S, Department of physics, Kanchi mamunivar center for post graduate studies, lawspet, Pondicherry-605 008.

Periandy. S, Department of physics, Kanchi mamunivar center for post graduate studies, lawspet, Pondicherry-605 008.

antioxidants, antidiabetics and cardiovascular agents, diuretics, hypoglycemic, hypolipidemic, antiarrhythmic and hypotensive agents. Due to the profound application as potential therapeutic agent in conjunction with synthetic accessibility and structural diversity, chromone group of compounds are often regarded as privileged scaffold in drug discovery and numerous reviews are available to justify a series of versatile synthetic methods involving them.

This present study aims to analyze both experimentally and theoretically the 3-cyano chromone compound by recording FTIR, FT-Raman, NMR and UV-Vis spectra and doing quantum chemical computations using DFT methods on the molecule. In this work the structural, conformational, and vibrational analysis of the compound are carried out by using B3LYP functional. The electron density (ED) in various bonding and anti-bonding orbital and stabilisation energies are predicted by Natural Bond Orbital (NBO) analysis. The UV spectroscopic studies along with HOMO-LUMO analysis have been used to explain the charge transfer within the molecule. In addition Docking analysis were also carried out using Auto-dock software to understand the biological activity of the compound.

II. METHODS

A. Experimental details

The 3-cyanochromone compound is purchased from Tokyo Chemical Industry (TCI) Co., Ltd., Tokyo, Japan. Chemical which is of spectroscopic grade and hence used for recording the spectra as such without any further purification. The NMR ^{13}C & ^1H spectra were recorded in the range of 20-200 & 1-10ppm respectively, with the scanning interval of 20 ppm in CdCl_2 solvent phase. The FT-IR spectrum was recorded by KBr pellet method on a Burker IFS 66V spectrometer in the range of 4000- 400 cm^{-1} with the spectral resolution of 2 cm^{-1} . The FT- Raman spectrum was also recorded in the range of 4000- 100 cm^{-1} using the same instrument with FRA 106 Raman module equipped with Nd: YAG Laser source operating at 1.064 μm with 200 mW powers and Ge detector. The frequencies of all sharp bands are precise to 2 cm^{-1} . The UV spectrum of the titled compound is recorded with the UV-1700 spectrophotometer. The spectrum is recorded for the spectral wavelength range of 200- 400 nm with a scanning interval of about 0.2nm.

B. Quantum chemical calculations

All the computations on the molecule 3-cyanochromone were performed using the GAUSSIAN 09 software [12] on Pentium IV processor in personal computer. The geometry of the titled compound was optimized using B3LYP functional in combination with cc-pVDZ basis set. The NMR chemical shift was carried out by GIAO method in

combination with B3LYP functional and cc-pVDZ basis set. In addition, Mullikan charges and natural charges of the title molecule are also computed using B3LYP method with same basis set. The optimized parameters of the compound 3-cyanochromone were used for harmonic vibrational frequency calculations, resulting in FT-IR and FT-Raman frequencies together with intensity and Raman depolarization ratios. The electronic properties such as NBO and HOMO-LUMO of the titled compound were calculated using time-dependent TD-SCF method under the same functional and basis set. From the theoretical calculations the optical properties of the titled compounds such as dipole moment, polarizability and hyper polarizability were predicted.

III. RESULT AND DISCUSSION

3.1 Conformational analysis

The optimized molecular structure of the present molecule was used for conformational analysis, which was performed by potential energy surface scan techniques using B3LYP, by varying the dihedral angle 20H-18N-17C-22H in the steps of 10 $^{\circ}$ over one complete rotation. The graphical result, total energy (Hartree) verses scan coordinates of the conformer, is presented in Fig 1. The graph clearly shows that conformer at minimum energy level occurs at 175 $^{\circ}$, with energy value -0.0553 Hartree. This conformer serves as the most stable conformer of the compound. The maximum energy is observed for the conformer at 225 $^{\circ}$ with energy value -0.0523 Hartree, this is the least stable or most unstable conformer of the compound. The most stable conformer is used for all the computational analysis in the present work.

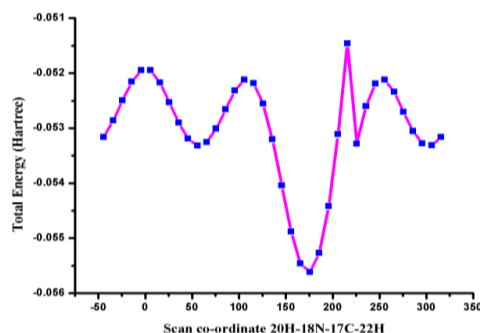


Fig. 1 The potential energy curve of 3-Cyano chromone

3.2 Molecular geometrical analysis

The structural analysis of 3-cyano chromone was carried out using B3LYP method and cc-PVDZ basis set for the most stable conformer of the compound. The bond lengths and bond angles of the compound calculated using this method are listed in the Table1. The optimized structure of the compound is shown in Fig 2. The experimental data obtained through single crystal X-ray method for title molecule

reported at an earlier work [13] was used here for the comparison purpose. The theoretical values indicate that the most of the bonds lengths are slightly higher in magnitude than that of the experimental values.

This compound has ten C-C, five C-H, three C-O, and one C-N bonds. The C-C single bonds are expected to value around 1.45Å and the C=C double bond around 1.35 [14]. In the present molecule, in benzene ring, all the CC bonds have bond length values between 1.38 Å -1.40 Å. This shows they are neither single bonded nor double bonded, which is due to the conjugation of the electrons among these bonds. The variation in values among them is due to the distribution of electron density within the ring among these bonds. In the case of pyrone ring, the C4-C9 and C9-C12 bonds are found to have length of 1.48Å, this value is higher than the expected range for even CC single bond, which may be due to the presence of oxygen atoms in this ring. The tendency of oxygen atom is to attract an electron towards itself, hence it redistributes the occupancy of electrons present within this ring. The bond length between C12-C13 is 1.36 Å, which is slightly greater than the CC double bond value, this may be due to the presence of cyano group at C12 and also due to oxygen atom attached in C13 atom.

According to the literature [15], the CO single bond and double bond are expected to have values 1.35 Å and 1.22Å respectively. In the present compound, the CO found at C9-O15 has bond length 1.22 Å, which indicates that it is clearly a double bonded, where as other C-O bonds, C3-O16 and C13-O16 are found to have values 1.38 Å and 1.35 Å respectively, which are single bonded but slightly deviated from the expected value, which may be due to the conjugation present in the pyrone ring.

All the CH bonds in the benzene ring structure are expected to be of length 1.08 Å [16]. In the present compound, CH bonds are having the bond length values between 1.082 Å to 1.088 Å. There is only one C-H in pyrone ring which is found to be 1.088 Å, whereas all other are in benzene ring whose values are closer to expected value. The slight variation is purely due to the changed conjugation of these two rings due to their fusion.

The chromone has only one cyano group. The bond length of the C12-C17 is 1.43 Å, which is a single bond CC. The C17-N18 has a bond length value of 1.15 Å, it implies the expected triple bond formation happens between C&N atoms.

The bond angle around each carbon atom is expected to be 120°[17]. In this molecule the bond angle between C2-C1-C6 single bond and C2-C4-C9 single bond angle are observed to be 120° as expected, but the other bond angles are varying between 117°-122°, which means the bond angle are deviated from the expected value due to the influence of O atoms and CN group in the pyrone ring.

The same 120° angles are expected for all the CCH bonds, but a small variation of the bond angles are observed between the CCH bonds, which are due to the variation of electronic conjugation among the CCC bonds. All these CCC single bond and CCH single bond angles indicate that the structure of the chromone rings are slightly distorted due to the presence of oxygen and CN group in the molecules.

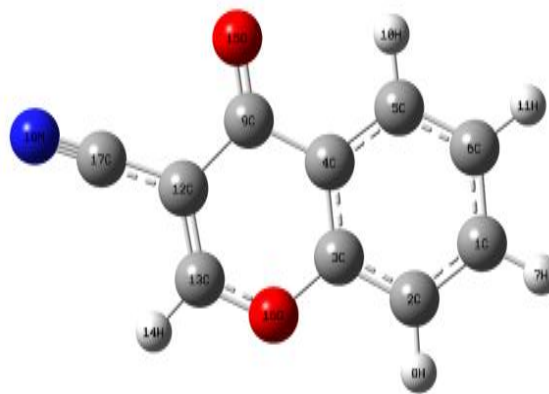


Fig.2 Structure of 3-Cyano chromone

3.3 Mullikan and Natural charge analysis

The atomic charge analysis plays important role in the prediction of the properties of the molecule, as the atomic charges affect parameters such as dipole moment, molecular reaction, Vibrational frequency, NMR chemical shift, etc [18,19]. The atomic charges are calculated by two methods in the present case for comparison purpose; Mullikan Population Analysis (MPA) and Natural Atomic Charges (NAC), by B3LYP/cc-pVDZ method and the values are listed in the Table 2 and the graphical representation shown in the fig.3.

Carbon atoms in the benzene ring C1, C2, C3, C4, C5, C6, are expected to be equally negative except C3 & C4, as the pyrone ring is fused at this bond, but they are predicted to be positive except C3 in MPA and negatively charged in NAC. The atom C3 is having negative value (-0.32) in MPA and positive value (0.33) in NAC. C3 in the molecule is found attached to O atom in the pyrone ring, hence it can be positive as predicted by NAC, as the O atom is more electro negative than C. The C4 is predicted by highly positive 2.910 in MPA, while slightly negative -0.18714 in NAC. The C4 atom is attached to C=O group in the pyrone ring, hence all its charge cannot be dragged, as O is not directly connected, which indicate the NAC prediction is reasonable. Rest of the C atoms C1, C2, C5 & C6 are not influenced by the presence of O&N atoms in substitutional groups, hence they are expected to be equally the presence of O&N atoms in substitutional groups, hence they are expected to be equally

Carbon atoms present in the pyrone ring are C9, C12, C13 and C17, in which C9 (-0.046) and C17

(-0.8191) are negative in MPA and positive charge in the NAC, again these two atoms are attached with O atoms in the ring, hence they can only be positive not negative as predicted by MPA.

C17 is the carbon atom present in the cyanide group, hence it can be slightly negative but not positive as predicted by NAC. The C13 has the positive values in the both MPA and NAC. This positive result found due to the presence of oxygen atom in this carbon atom. N18 atom has the moderate charge due to the nature of electronegativity. The nitrogen atom having negative charge on both MPA (-0.1953) and NAC (-0.3049) because of it has more electronegativity than carbon atom. All hydrogen atoms are having a negative charge in MPA and positive in NAC. The NAC prediction in this case is reasonable as the H atoms can only lose electrons to the C atoms to which they are attached, as C atoms are more electronegative compared to H atoms.

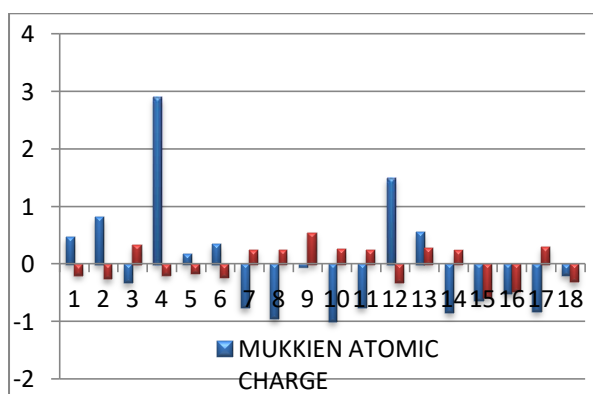


Fig. 3 Mulliken and natural atomic charges of 3-cyano chromone

3.4 NMR Chemical Shift Assessment

The Experimental and theoretical values of ^1H NMR and ^{13}C NMR chemical shift of 3-cyano chromone are presented in Table 3. Chemical shifts are calculated in ppm and relative to TMS for ^1H NMR and ^{13}C NMR spectra. The optimization of the 3-cyano chromone was performed in density functional theory using the hybrid of B3LYP with the basis set cc-pVDZ method, supported by Gauge Including Atomic Orbital (GIAO) technique for finding ^1H and ^{13}C chemical shifts.

Aromatic carbons give the spectrum with chemical shift values from 120-130ppm [20]. The experimental chemical shifts in the benzene ring are C1(123.4ppm), C2 (102.9ppm), C3(155.8ppm), C4 (118.5ppm), C5 (118.5ppm), C6 (112.3ppm). The computed chemical shift for carbon atoms C3, C4 and C5 in solvent phase are (147.7ppm), (117.1ppm) and (117.7) respectively. The experimental values are slightly deviated from the theoretical values. Only C1 is in expected range, all other C atoms are found to have slightly less value compared to the expected range. The C3 atom shows the highest value which is in accordance with charge prediction, highly positive,

by NAC method, due to the presence of O atom in the pyrone ring. Since C4 is not attached directly with O atom, its value is found to be slightly less than the expected value, which shows it is slightly deshielded, as observed by NAC method. The same reason can also be attributed to C2 (102.9ppm) and C6 (118.5ppm), as their values are also slightly less than the expected range.

In the pyrone ring, there are two O atoms and one N atom, which are more electro negative than carbon atoms. Therefore C9 (162.4ppm) and C13 (135.4ppm) which are directly attached to O atom share values greater than the expected range. C12 has the chemical shift value (123.4ppm) within the expected range, as it is not directly connected to either O or N atoms. C17 which is connected to N atom (in Cyano group) is found to have very less value 102 ppm, this is possible because it is not present within the ring where there is a possibility for conjugation, but it is present outside the ring like an aliphatic group. Hence, the chemical shift value must be around 45-65 ppm like methyl/ ethyl carbon, since it is connected to N atom its shift is enhanced closer to aromatic carbon.

The chemical shift value of ^1H atoms in benzene ring is expected between 7.0-8.0 ppm [10]. The chemical shifts obtained in this case are found in between 7.805-8.435ppm. Only the two H atoms in the pyrone ring are found to have values greater 8 ppm, which is naturally due to the presence of O atoms. The H atoms in the benzene rings are very well within the expected range which shows whose charge distribution is not disturbed by the pyrone ring.

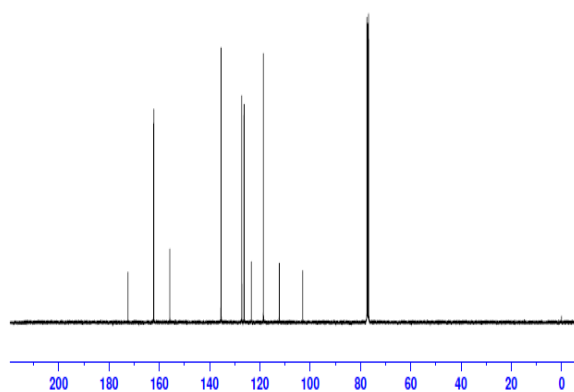


Fig. 4 ^{13}C NMR Experimental spectrum of 3-Cyano chromone

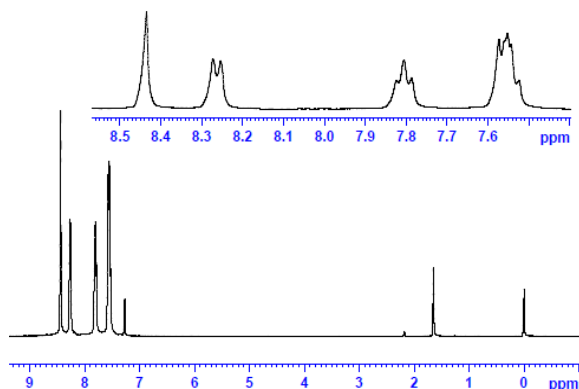


Fig. 5 ¹H NMR Experimental spectrum of 3-Cyano chromone

3.5 Vibrational Analysis

The 3-cyano chromone, the molecule under investigation has 18 atoms and 48 normal modes of fundamental vibrations. Vibrational wave numbers for all the modes were computed using DFT (B3LYP) methods with cc-pVDZ basis sets and the values along with the experimental values are presented in table 4. The experimentally recorded and theoretically constructed FT-IR and FT Raman spectra of the 3-cyano chromone compound are shown Fig.6 and 7 respectively.

The calculated wave numbers are found slightly higher than the observed values for the majority of the normal modes. Two factors may be responsible for the discrepancies between the experimental and computed wave numbers; the first is caused by the unpredictable electronic distribution among the different bonds in the molecule and the second reason is the anharmonic nature of the vibrations which cannot be accounted completely by theory. Scaling strategies were used to bring computed wave numbers to coincide with observed values. In this, study, the scaling factor used is 0.956 in accordance with earlier work on similar molecules [21, 22].

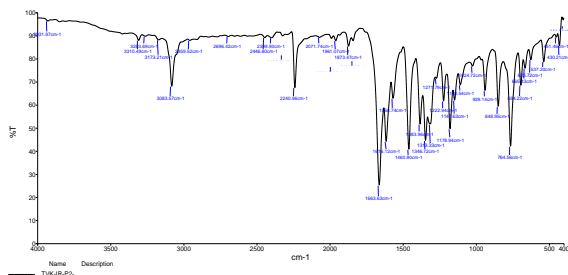


Fig. 6 Experimental FT-IR spectra of 3-Cyano chromone

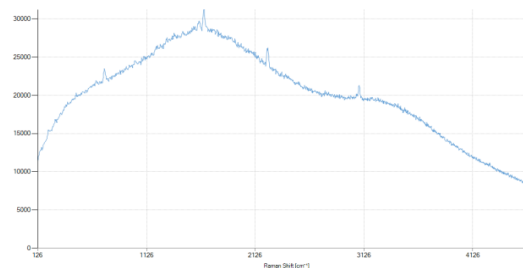


Fig. 7 Experimental Raman spectra of 3-Cyano chromone

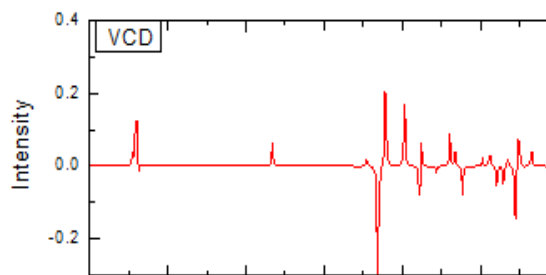


Fig. 8 VCD spectra of 3-Cyano chromone

C-H vibrations

The aromatic structure represents the presence of C-H stretching vibration in the characteristic region of 3100-3000 cm⁻¹[23]. The C-H stretching modes are usually appears with the strong Raman intensity due to their high polarization. In the present study, the stretching vibrations are predicted at 3183 cm⁻¹, 3171 cm⁻¹, 3168 cm⁻¹, 3157 cm⁻¹, and 3144cm⁻¹. In the experimental study, the aromatic C-H stretching vibrations were observed at 3263cm⁻¹, 3173 cm⁻¹ in FT-IR and 3219 cm⁻¹, 3200 cm⁻¹, 3188 cm⁻¹ in FT-RAMAN respectively. All these values are above the limits meant for aromatic CH, which indicate the pyrone group has greatly influenced these CH stretching modes, due to the presence of O and N atoms.

The C-H in plane bending modes usually occurs as strong to weak bands in the region of 1000 cm⁻¹ [24]. Experimental study of this compound manifested C-H in plane bending vibration in the region of 1147 cm⁻¹, 1024 cm⁻¹ and 981 cm⁻¹in FT-IR spectrum and 1126 cm⁻¹and 1015 cm⁻¹in FT-Raman spectrum.

The C-H out of plane bending vibrations are expected to strong to weak intensity bands in the region of 1000-750 cm⁻¹ [25]. Their frequency depends on the number of adjacent hydrogen atoms in the ring system but they are not significantly affected by the nature of substituents. The recorded FT-IR spectrum of this molecule showed bands at 848 cm⁻¹, 764 cm⁻¹while its FT-RAMAN spectrum manifested bands at 888 cm⁻¹, 820 cm⁻¹, cm⁻¹, 782 cm⁻¹, 735 cm⁻¹. Their corresponding computed values were noted at 884 cm⁻¹ to 743 cm⁻¹respectively.

The C-C-H torsion vibrations are appeared at 408cm⁻¹, 374cm⁻¹, 287cm⁻¹ respectively and the FT-IR can be observed at 404cm⁻¹.

C=C and C-C vibrations

The C-C stretching vibrations are very much important in the spectrum of benzene and also pyrone.

In the benzene ring, the C=C and C-C stretching vibrations are generally observed between 1600 cm⁻¹ to 1500 cm⁻¹ and 1500 cm⁻¹ to 1400 cm⁻¹[26]. In the present compound the benzene ring C=C and C-C stretching vibration were appeared at 1635cm⁻¹, 1624cm⁻¹, 1473cm⁻¹, 1463cm⁻¹, 1370cm⁻¹, and 1360cm⁻¹ by B3LYP/cc-pVDZ method. In recorded spectrum, these are at 1663cm⁻¹, 1661cm⁻¹, 1460cm⁻¹, 1383cm⁻¹ in FT-IR and 1497cm⁻¹, 1411cm⁻¹ and 1376 cm⁻¹ in FT RAMAN. All the CC vibration in the benzene ring was within the observed range.

In the pyrone ring, the C=C and C-C stretching vibration is observed in the region of 1586cm⁻¹ and 13317cm⁻¹, 1263cm⁻¹ respectively. In experimentally, C=C and C-C stretching is appeared at 1568 cm⁻¹, 1346 cm⁻¹, 1271 cm⁻¹ in FT IR spectrum.

The C-C stretching vibration in the external group of cyano group can be observed at 1222cm⁻¹ and the FT IR spectrum of C-C is appeared at 1222cm⁻¹. The C-C out of plane bending can be founded at 694cm⁻¹ in the FT-IR.

The C-C-C in plane bending in trigonal vibration mode in molecule can be founded at 242 cm⁻¹, 214cm⁻¹, 132 cm⁻¹, 130 cm⁻¹ and 62 cm⁻¹ in the computed values.

C=O and C-O Vibrations

In C-O group, the absorption is sensitive for both carbon and oxygen atom. Normally the C-O stretching vibration occurs in the range 1150cm⁻¹[27]. The intensity of the chromone group increases due to the conjugation or formation of hydrogen bonds. The increases in conjugation, which increases the intensity of Raman lines as well as the IR band intensities. According to the above facts, there are two theoretical wave numbers are observed in the pyrone ring at 1178cm⁻¹ and 1169cm⁻¹. The corresponding experimental FT RAMAN bands were observed at 1190cm⁻¹ and FT-IR is appeared at 1178cm⁻¹. The torsion C-C-O bending vibration mode is appeared at 501cm⁻¹ in FT RAMAN and 451m⁻¹ in FT IR, hence the calculated mode at 484cm⁻¹ and 455 FT cm⁻¹ respectively.

The stretching mode of C=O in the pyrone ring is expected in the range at 1750cm⁻¹[18]. The theoretical study this title compound showed only one C=O stretching band at 1703cm⁻¹ with PED contribution of 83%. In experimentally the FT RAMAN spectrum was observed at 1751cm⁻¹. The C=O in plane bending mode is founded at 927cm⁻¹ in the computed values and the corresponding FT-IR

spectrum of C=O in plane bending appeared at 939cm⁻¹. The C=O out of plane bending vibration in FT IR spectrum can be observed at 665cm⁻¹ and the calculated value at 665cm⁻¹. The C-C=O torsion bending were computed at the range of 549cm⁻¹ and 534cm⁻¹ respectively. The experimental FT-RAMAN and FT-IR values are obtained at 560 cm⁻¹ and 537 cm⁻¹.

C≡N Vibrations

In this titled molecule stretching vibrations of C≡N vibration mode was observed in 2300cm⁻¹ in the computed value and the FT IR spectra were founded in 2240cm⁻¹. The in-plane bending have the range at 711cm⁻¹ in the calculated value and the corresponding experimental in plane vibration at 694cm⁻¹ is observed in FT-IR spectra. The out of plane bending of CN is computed in the range 527cm⁻¹ and in FT-RAMAN is 511cm⁻¹.

The C-C≡N out of plane bending vibration can be calculated by the computed values is 427cm⁻¹, then FT-IR obtained at 430 cm⁻¹ and Ft-RAMAN is 423 cm⁻¹ respectively.

3.6 NBO Analysis

The bonding and non-bonding (anti-bonding) interactions can be quantitatively described in terms of the NBO (Natural bonded orbitals) analysis, which can be predicted by in terms of the second order perturbation interaction energy [E⁽²⁾][28, 29]. This energy represents the estimation of the off diagonal NBO Fock matrix elements. It can be deduced from the second order perturbation approach [30]

$$E^{(2)} = \Delta E_{ij} = q_i \frac{F(i, j)^2}{\epsilon_j - \epsilon_i}$$

Where,

Q_i is the donor orbital occupancy, ε_i and ε_j are diagonal elements (orbital energies) and F(i,j) is the off diagonal NBO Fock matrix elements.

In this analysis, the occupancies, from bonding to anti-bonding levels, and their energy levels were calculated and presented in the Table 5. The highly probable π-π* and n-π* transitions are observed between C-C, C-O, & C-N bonding orbitals with adjacent anti-bonding orbitals. The highest π-π* transitions in 3-cyano chromone based on the E2 values in descending order can be listed as C1-C2 to C3-C4 (π-π*, 22.29 kcal/mol), C5-C6 to C1-C2 (π-π*, 21.56 kcal/mol), C3-C4 to C9-O15 (π-π*, 20.58 kcal/mol), C5-C6 to C3-C4 (π-π*, 18.83 kcal/mol), C3-C4 to C1-C2 (π-π*, 16.41 kcal/mol), and C1-C2 to C5-C6 (π-π*, 16.26 kcal/mol).

The highest π-π* stabilization energies in pyrone ring are C12-C13 to C9-O15 (π-π*, 21.38 kcal/mol), C12-C13 to C17-N18 (π-π*, 17.77 kcal/mol) and the n-π* stabilization energies are O16 to C12-C13 (n-π*, 35.74 kcal/mol), O16 to C3-C4 (n-π*, 25.27 kcal/mol), O15 to C9-C12 (n-π*, 21.95 kcal/mol), O15

to C4-C9 ($n-\pi^*$, 19.87 kcal/mol), and N18 to C12-C17 ($n-\pi^*$, 12.47 kcal/mol).

Therefore the top ten highly probable electronic transitions, according to their stabilization energy can be listed as follows: 1. O16 to C12-C13 ($n-\pi^*$, 35.74 kcal/mol), 2. O16 to C3-C4 ($n-\pi^*$, 25.27 kcal/mol), 3. C1-C2 to C3-C4 ($\pi-\pi^*$, 22.29 kcal/mol), 4. O15 to C9-C12 ($n-\pi^*$, 21.95 kcal/mol), 5. C12-C13 to C9-O15 ($\pi-\pi^*$, 21.38 kcal/mol), 6. C3-C4 to C9-O15 ($\pi-\pi^*$, 20.58 kcal/mol), 7. O15 to C4-C9 ($n-\pi^*$, 19.87 kcal/mol), 8. C5-C6 to C3-C4 ($\pi-\pi^*$, 18.83 kcal/mol), 9. C3-C4 to C1-C2 ($\pi-\pi^*$, 16.41 kcal/mol), and 10. C1-C2 to C5-C6 ($\pi-\pi^*$, 16.26 kcal/mol). All these transitions though theoretically favorable, only a few transitions will be allowed by the selection rules, which can be identified by the oscillator strength and HOMO- LUMO contribution, as it is done in the following section.

3.7 UV-Visible Analysis

The UV-Visible spectrum of the 3-cyano chromone is recorded in the range of 200-400 nm in Ethanol solvent phase [31]. The theoretical UV-Vis studies which analyze various possible electronic excitation, wavelength, oscillation strength and also major FMO contribution in both gas phase and an ethanol phase is carried out using TD-SCF method along with B3LYP/CC-PVDZ combination, all these parameters both experimental and theoretical are presented in Table 6.

The theoretically simulated spectrum in ethanol phase shows a broad hump over the wavelength region between 309 nm to 202 nm with energy gap ranging from 3.642 eV to 5.472 eV. However, the oscillator strength and HOMO to LUMO contribution shows that only the second transition in the list O16 to C3-C4 ($n-\pi^*$, 25.27 kcal/mol) causes the peak value in the hump. This value indicates that this is a $n-\pi^*$ transition which takes place at the wavelength 289 nm theoretically and 270 nm experimentally. The other transitions which have considerable oscillator strengths value among $\pi-\pi^*$ transitions, are the sixth and seventh transition in the list C3-C4 to C9-O15 ($\pi-\pi^*$, 20.58 kcal/mol), and O15 to C4-C9 ($n-\pi^*$, 19.87 kcal/mol), but the HOMO – LUMO contribution for this transition are found to be very low, hence these transitions cannot take place in the spectrum. But, indeed these transitions have appeared in the spectrum at wavelength 234 and 228 nm, which may be due to the fact that all these transitions originate from the same location in the molecule.

The same trend is also observed in gas phase also, except a small difference in absorption wavelength. The sixth transition which is found active in ethanol phase is found inactive in gas phase. These two observations may be attributed to the solvent effect in this molecule. The major contributions of the transitions were designated with the aid of SwiZaed

program [23]. From the calculated absorption spectra, the maximum absorption wavelength corresponds to the electronic transition from the HOMO to LUMO with 88% contribution in gas phase and from HOMO-LUMO 91% contribution in ethanol phase. The other major contribution of various wave lengths are listed in the table 6.

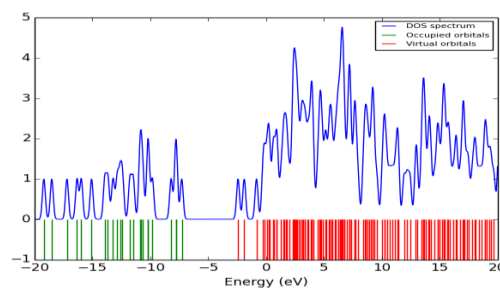
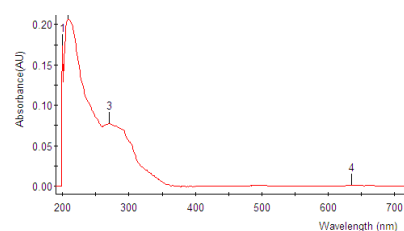
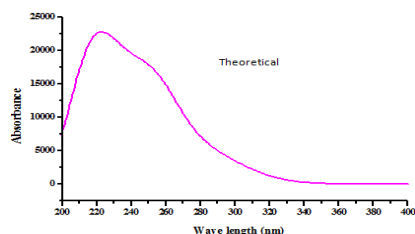


Fig. 9 Theoretical and Experimental UV-Vis and DOS Spectra of 3-Cyano chromone

3.8 HOMO-LUMO Analysis

The highest occupied molecular orbital (HOMO) donates electrons while the lowest unoccupied molecular orbital (LUMO) accepts electrons from the orbitals. These orbitals are known as frontier molecular orbital. The frontier molecular orbitals are very much useful for studying the electric and optical properties of the organic molecules. The energy gap (eV) between the HOMO and LUMO is very important parameter to study the chemical behavior of a compound [32][33]. Also, the energy gap between HOMO-LUMO of the molecules determines whether it can have high reactivity or low kinetic stability [34]. The calculated HOMO and LUMO energies of the 3-cyano chromone molecule was found to be -0.2734 and -0.0247, respectively, using the DFT method of B3LYP with the basis set of CC-PVDZ and the energy gap between HOMO-LUMO was -0.2095 eV. The HOMO-LUMO energy gap and different reactivity descriptors of molecule in both levels are presented in the table. The negative charge was represented as red and the positive charge was represented by green colour. It showed the

spread of HOMO over the chromone ring of oxygen and some part of the chromone ring while LUMO was located. The HOMO-LUMO energy gap reveals the unlimited possible charge transfer within the molecule and hence its possible chemical and biological reactivity with respect to the transition, there are ten maximum computed wavelengths 309.94, 289.84, 268.78, 254.86, 254.27, 234.97, 228.32, 215.58, 205.52, 202.91nm, which correspond to the major contribution of H-1->LUMO (95%), HOMO->LUMO (91%), H-2->LUMO (43%), H-2->LUMO (48%), H-1->L+1 (97%), H-3->LUMO (82%), H-3->L+1 (16%), H-3->L+1 (50%), H-1->L+2 (98%), H-3->L+1 (11%) in the solvent phase. The transition can be accounted for the non-bonding transition (n- π^*) of the lone pair in the molecule. Frontier molecular orbital of 3-cyano chromone is shown in the fig.10.

In this study of molecule have been calculated some values such that Electronegativity, global hardness (η), Global softness (s), Electrophilicity index (ω), Dipole moment (μ). According to Koopman's theorem [35] (E_{HOMO}) is represents Ionization Potential (IP) and (E_{LUMO}) is represents Electron Affinity (EA).

Electronegativity (χ):

The electronegativity is defined by Mullikan as the average of ionization potential (IP) and electron affinity (EA)[36].

$$\chi = -\frac{1}{2}(E_{\text{H}}+E_{\text{L}})$$

Global Hardness (η):

The hardness of a molecule is related to the gap between the HOMO and LUMO orbital's. The larger HOMO-LUMO energy gap the harder will be the molecule chemical hardness can be calculated as follows [37]

$$\eta = -\frac{1}{2}(E_{\text{H}}-E_{\text{L}})$$

Global Softness (s)

The global softness is the inverse of global softness [38]

$$S = -2(E_{\text{H}}-E_{\text{L}})$$

Electrophilicity Index (ω)

Parr et al., have introduced global electrophilicity index which measures the propensity of a species to accept electrons. It can be calculated by using the electronegativity (χ) and chemical hardness (η) [39]

$$\omega = \frac{\chi^2}{2\eta}$$

The electronegativity is a measure of attraction of an atom for electrons in a covalent bond has found to be 0.1490. The global hardness is a measure the resistance of an atom or a group of atoms to receive electrons and is equal to reciprocal of global hardness and it is found to be 0.2430. The global softness describes the capacity of an atom or a group of atoms to receive electrons and is equal to reciprocal of global hardness and it is found to be 0.4974. The electrophilicity index is a measure of lowering of total energy due to the maximal electron flow between the

donors and the acceptors and it is found to be 0.0893. The dipole moment is found to be 7.5593.

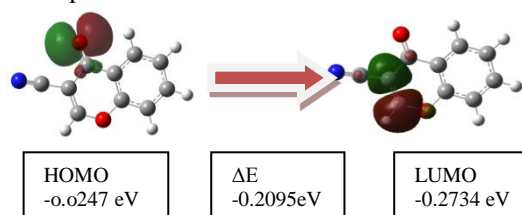


Fig. 10 Frontier molecular orbitals of 3-Cyano chromone

3.9 NLO Properties

Organic and semi-organic NLO materials have been subjected to intense research due to their possible applications in wide range of technologies, such as optical communication, optical computing and data storage, etc. The first order hyperpolarizability is a third rank tensor that can be described by a $3 \times 3 \times 3$ matrix. The 18 components of the 3D matrix can be reduced to 10 components due to Kleinman symmetry [40]. The total static dipole moment (μ), the mean polarizability (α_0) and the mean first order hyperpolarizability (β_0), using the x, y, z components are defined as

$$\mu = (\mu_x^2 + \mu_y^2 + \mu_z^2)^{1/2} \quad (1)$$

$$\alpha_0 = \frac{\alpha_{xx} + \alpha_{yy} + \alpha_{zz}}{3} \quad (2)$$

$$\beta_0 = (\beta_x^2 + \beta_y^2 + \beta_z^2)^{1/2} \quad (3)$$

$$\Delta\alpha = 1/\sqrt{2} [(\alpha_{xx}-\alpha_{yy})^2 + (\alpha_{yy}-\alpha_{zz})^2 + (\alpha_{zz}-\alpha_{xx})^2 + 6\alpha_{xy}^2 + 6\alpha_{xz}^2 + 6\alpha_{yz}^2]^{1/2} \quad (4)$$

$$\langle\beta\rangle = [(\beta_{xxx} + \beta_{yyy} + \beta_{zzz})^2 + (\beta_{zyy} + \beta_{yzz} + \beta_{yxx})^2 + (\beta_{zzx} + \beta_{zxy})^2]^{1/2} \quad (5)$$

The NLO properties of 3-cyano chromone compound were calculated using B3LYP/cc-PVDZ method. The electronic dipole moment (μ) (Debye), polarizability (α) and first hyperpolarizability (β) of 3-cyano chromone are given in table 8. Standard value for urea ($\mu=1.3732$ Debye, $\beta_0=1.584 \times 10^{-30}$ esu): esu-electrostatic unit. The dipole moment (μ) and first order hyperpolarizability (β_0) values are calculated at 7.5599 Debye and 167.24×10^{-33} esu, respectively. These results show that, the β_0 values of studied molecules are higher than the magnitude of urea which is used frequently as a threshold value for comparative purposes [41,42]. This high value of hyperpolarizability may be due to the presence of electro-negative nitro group and π bonds. The theoretical calculation of β components is very useful as this clearly indicates the direction of charge

delocalization. Domination of particular component indicates on a substantial delocalization of charges in this direction. The β_{xxx} direction shows largest value of hyperpolarizability which insists that the delocalization of electron cloud is more that direction than other directions. Therefore, the largest β_{xxx} value indicates charge delocalization is perpendicular to the bond axis and the involvement of π orbitals in intra-molecular charge transfer process. Hence the molecule has good NLO activity.

3.10 MEP (molecular electrostatic potential) Analysis

The molecular electrostatic potential (MEP) is related to the electron density and is a very useful parameter to understanding sites for electrophilic and nucleophilic reactions as well as hydrogen bonding interactions [43, 44]. The different values of MEP surface are represented by different colors: red, blue and green represent the regions of most negative, most positive and zero electrostatic potential, respectively. The red color represents negative electrostatic potential corresponds to an attraction of the proton by the aggregate electron density in the molecule, while the positive electrostatic potential corresponds to a repulsion of the proton by the atomic nuclei (blue). From the MEP surface is evident that the negative charge covers the C=O group and C≡N group and the positive region is over the remaining part of the chromone group in the titled compound. The MEP surface of the title molecule is shown in Fig.11.

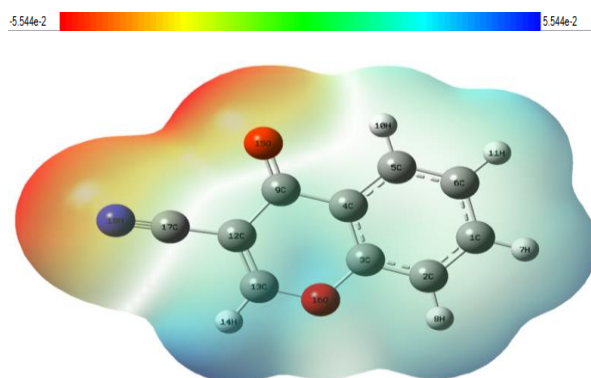


Fig. 11 MEP surface of 3-Cyano chromone

3.11 Thermodynamic properties

The thermodynamic functions of this 3-cyano chromone compound at different temperatures were calculated at B3LYP/cc-pVDZ level and were listed in the Table 9. The entropy, specific heat capacity and enthalpy were varied with respect to temperature from 100K to 300K. The variation of the parameters was found to be linear and sustained up to the maximum temperature. This shows that the consistent chemical stability of this compound. Similarly, the Gibbs free energy was observed to be linear with respect to temperature. The chemical reaction can be possible when the Gibbs free energy of the molecular system

decreases. It indicates that the Gibbs free energy is negative or less than zero, the chemical reaction is continued. If it is positive, the reaction will be stopped. In this case, the Gibbs energy was found to be still negative up to 300K and it was concluded that, the present compound was chemically strong and active.

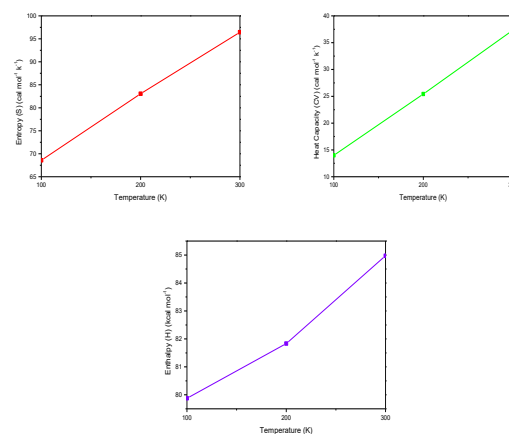


Fig. 12 Correlation graph of thermodynamic properties at different temperature of 3-Cyano chromone

3.12 Reduced Density Gradient (RDG) analysis

The RDG is obtained from electron density as a dimensionless quantity of its first gradient was developed [45].

$$RDG(r) = \frac{1}{3(3\pi r^2)^{3/2}} + \frac{\Delta^2 \rho(r)}{\rho(r)^{5/2}}$$

The plot of $\rho(r)$ in x-axis and λ_2 in y-axis provides the nature and strength of interaction in the molecule using color code interaction. The RDG analysis was carried out by an isosurface, steric effect and H-bond is plotted by using Multiwfn software [46]. The steric effect is representing the strong repulsion and H-bond, isosurface are strong attracted that appear in the ring system and the strong Vander Walls interaction are located in cyano and C=O atom in the ring system.

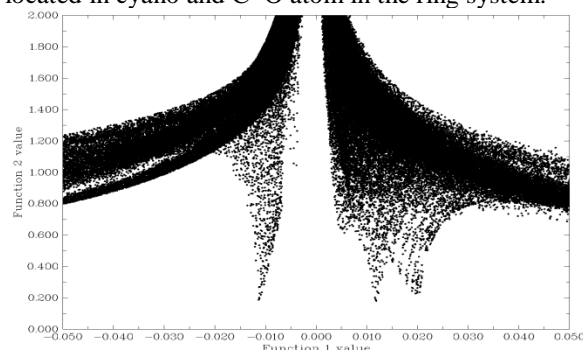


Fig. 13 Reduced Density Gradient of 3-Cyano chromone

3.13 Electron Localization Function (ELF) analysis

Electron localization function analysis represent $n(r)$ is scalar function and Fermi hole curvature [47]. In this calculation were found at kinetic energy density using Pauli relation. In present graphical 2D & 3D image representation fig 14, illustrated using Multiwfn software [46]. These atoms play an important role in the determined denote the surface of core i.e. blue colour represent neutral charge red color hole represent negative charge covers the C=O group and C≡N group. The positive region is over the reaming part of the chromone group in the titled compound.

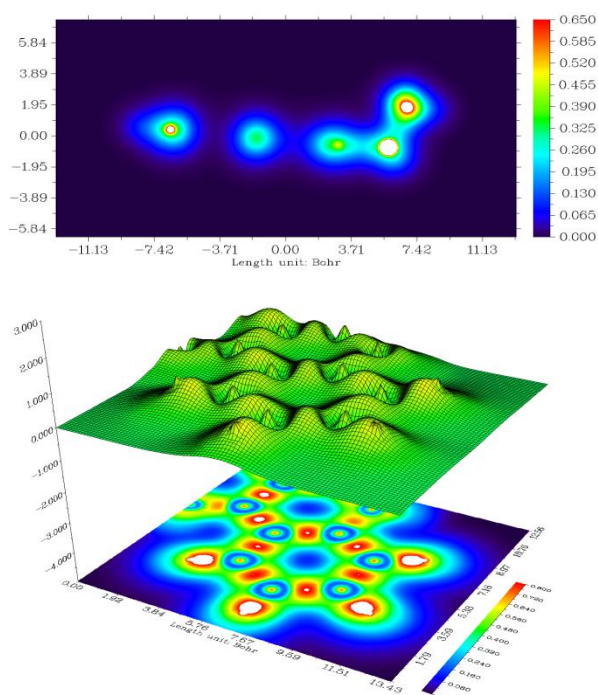


Fig. 14 2D & 3D Electron Localization Function of 3-Cyano chromone

3.14 Docking Analysis

The normal resolution crystal structure of Human SULT1A1 bound to PAP protein was used as a target protein in (protein ID: 3U3M) [48] and auto dock 4.0 software package [49] was utilized to perform docking study. The protein structures were prepared with the help of Auto dock tools graphical [49] user intergace. polar hydrogen was added to the protein, atomic charges calculation kollman method and Lamarckian genetic Algorithm (LGA) were utilized auto dock package.

In our protein data bank molecule (ligand) was created by using optimized molecule. The energies were defined to add residues of active side with the use of grid size $90\text{\AA} \times 90\text{\AA} \times 90\text{\AA}$ using Auto grid. The

Lamarckian Genetic Algorithm is implemented in Auto dock were employed for docking [49].The Auto dock binding energy (kcal/mol), inhibition constants, intermolecular energy were computed and Tabulated in Table 10, the best lowest energy docked position of the ligand with protein are illustrated in Fig.15.

The best result i.e. lowest binding result are shown in 3U3Mprotein exhibit the lower binding energy (5.52 kcal/mol) with inhibition constant value of $89.53(\mu\text{m})$. The analysis shows the PHE 81 form H-bond with cyano group existence of the protein-ligand interact with the bond length of 3.0\AA and PRO 90 form H-Bond with C=O existence of the protein-ligand interact with the bond length of 3.1\AA . Here, structural, protein and ligand were employed to obtain deep understanding of the molecular basis for the broad specificity and substrate inhibition of SULT1A1. We found that active site binding of protein-ligand site active in hydrogen bonding for food resolution.



Fig. 15 Docking analysis of 3-Cyano chromone

IV. CONCLUSION

The molecular spectroscopic and the theoretical tools were properly used to predict the physical, chemical and biological properties of the compound 3-cyano chromone and following observation and conclusion are made;

The optimized structure of the title compound was performed using B3LYP/cc-pVDZ basis set compare with the XRD values are determined the most stable conformer of the compound, Such as C-C, C-H, C-O and C-N.

The NMR analysis, ^{13}C NMR chemical shift values of benzene ring shows 120-130ppm. The values are slightly varied due to the pyrone ring in that benzene ring. In the pyrone, the chemical shift founded at 164.8ppm in theoretical and 162.4ppm in experimentally. The ^1H NMR chemical shift in both benzene and pyrone ring appeared to be at 7 to 8 ppm.

The FT IR and FT RAMAN spectra of 3-cyano chromone have been recorded and the detailed vibrational harmonic frequencies, PED assignments are compared with the experimental data. Considerable level of correlation has been noticed. The detailed PED% analysis of the compound showed a good agreement with the experimental data.

The NBO analysis reflects the charge transfer occur within the molecule. In this study, the electronic transitions from bonding to antibonding levels were analyzed. The intermolecular hyper conjugative interactions are caused by the orbital overlapping between $\pi-\pi^*$ and $n-\pi^*$ (C-C, C-H, C-O and C-N) bonds orbital.

The UV-Visible spectra indicate that the entire electronic transition shifted bathochromically due to the substitutional effects. The calculated absorption maxima values have been founded to be in gas phase and the ethanol phase.

The calculated HOMO and LUMO along with their plot has been presented for understanding of charge transfer occurring with the compound. The HOMO and LUMO energies were used to semiquantitatively estimate the ionization potential, electronegativity, global hardness and softness, electrophilicity index and chemical potential.

The non-linear optical behavior of the molecule was predicted first order hyperpolarizabilities. The cyano functional group changes in the charge distribution both the inside and outside the pyrone ring causing large dipole moment and polarizability values.

The Molecular Electrostatic Potential founded the positive and negative electrostatic potential of the title compound. The electron density corresponds to an attraction and repulsion with the proton by the nuclei.

The thermodynamic parameter such as entropy, heat capacity and the enthalpy can be calculated using B3LYP/cc-pVDZ function. This parameter was performed by different temperature from 100K to 300K. The Gibbs free energy were calculated using the parameter and these values indicated that the compound chemically strong and active.

The docking analysis shows the PHE 81 form H-bond with cyano group existence of the protein-ligand interact with the bond length of 3.0 Å and PRO 90 form H-Bond with C=O existence of the protein-ligand interact with the bond length of 3.1 Å.

TABLES:

Table.1

Optimized Geometrical parameter 3-Cyano chromone
Computed at B3LPY/cc-pVDZ

Bond Length (Å)	XRD	Bond Angle (°)	XRD
Chromone ring (CC)		Chromone ring (CCC)	
C 1 - C 2	1.39 1	1.38 9	118. 5
C 2 - C 3	1.39 7	1.39 5	122. 1
C 3 -	1.40	1.39	118. 117.

C4	2	9	- C 5	2	7
C4 - C5	1.40 8	1.40 6	C -4 - C 5 - C 6	120. 4	121. 3
C 5 - C 6	1.40 8	1.37 8	C 2 - C 1 - C 6	120. 6	120. 6
C 1 - C 6	1.40 7	1.40 6	C 3 - C 4 - C 9	120. 6	120. 4
C4 - C9	1.48 2	1.47 7	C 5 - C 4 - C - 9	121. 1	121. 8
C 9 - C 12	1.48 1	1.46 4	C 1 - C 6 - C 5	120. 1	119. 5
C 12 - C 13	1.36 2	1.31 2	C 4 - C 9 - C 12	113. 2	113. 4
Cyano (CC & CN)			C 9 - C 12 - C13	120. 7	121. 2
C 12 - C 17	1.43 1	1.43 6	C 9 - C 12 - C17	120. 1	121. 1
C 17 - N 18	1.16 2	1.15 3	C 13 - C12 - C17	119. 1	-
Ring (CO)			Ring (CCO)		
C 9 - O 15	1.22 2	1.22 5	C 4 - C 9 - O 15	123. 4	123. 2
C 13 - O16	1.33 9	1.35 4	C 12 - C 9 - O 15	123. 2	123. 2
C 3 - O 16	1.38 2	1.37 1	C 2 - C 3 - O 16	116. 3	116. 1
Ring (CH)			C 4 - C 3 - O 16	121. 6	116. 1
C 2 - H 8	1.08 8	1.08 4	Ring (CCH)		
C 5 - H 10	1.08 8	1.08 3	C 1 - C 6 - H 11	119. 8	118. 7
C 6 - H 11	1.08 9	1.08 2	C 5 - C 6 - H 11	120. 1	121. 6
C 13 - H1 4	1.08 8	1.08 2	C 4 - C 5 - H 10	117. 7	117. 5
C 1 - H 7	1.09 1	1.08 2	C 3 - C 2 - H 8	119. 5	119. 4
			C 6 - C 5 - H 10	121. 7	121. 0
			C 6 - C 1 - H 7	119. 9	119. 9
			C 1 - C 2 - H 8	121. 9	121. 9
			C 2 - C 1 - H 7	119. 4	121. 0

Table.2

Charges of 3-Cyano chromone with B3LYP/cc-pVDZ basis set.

Atoms	B3LYP/cc-pVDZ	
	Mullikan Charge	Natural Charge

Benzene ring		
1 C	0.4682	-0.1901
2 C	0.8228	-0.2527
3 C	-0.3239	0.3343
4 C	2.9104	-0.1871
5 C	0.1830	-0.1617
6 C	0.3514	-0.2255
7 H	-0.7475	0.2402
8 H	-0.9523	0.2506
10 H	-0.9863	0.2617
11 H	-0.7452	0.2409
Pyrone ring		
9 C	-0.0464	0.5402
12 C	1.4948	-0.3196
13 C	0.5584	0.2813
14 H	-0.8396	0.2348
15 O	-0.6290	-0.5692
16 O	-0.5040	-0.4752
17 C	-0.8191	0.3018
18 N	-0.1953	-0.3049

Table.3

Calculated ^1H and ^{13}C NMR Chemical shifts (ppm) of 3-Cyano chromone

Atom	Gas	CdCl_2	Exp.
Benzene ring			
1C	123.5	125.4	123.4
2C	107.1	108.1	102.9
3C	147.3	147.7	155.8
4C	117.9	117.1	118.5
5C	118.7	117.7	118.5
6C	116.1	117	112.3
Pyrone ring			
9C	163.1	164.8	162.4
12C	96.01	93.62	123.4
13C	152.1	155.6	135.4
17C	101.4	104.4	102.9
Benzene ring			
7H	8.159	8.385	8.273
8H	7.953	8.157	7.805
10H	9.029	8.991	-
11H	8.072	8.239	7.822
Pyrone ring			
14H	8.773	9.044	8.435

Table.4

Vibrational Assignment

Experimental frequency cm^{-1}		Assignment	
FT-IR	FT-Raman	Scaled	Band
3263		3183	ν CH
	3219	3171	ν CH
	3200	3168	ν CH
	3188	3157	ν CH
3173		3144	ν CH
2240	2235	2300	ν CN
	1751	1703	ν C=O
1663		1635	ν C=C
1616		1624	ν C=C
1568		1586	ν C=C
	1497	1473	ν C-C
1460		1463	ν C-C
	1411	1370	ν C-C
1383	1376	1360	ν C-C
1346		1317	ν C-C
1271		1263	ν C-C
1222		1222	ν C-C
	1190	1178	ν CO
1178		1169	ν CO
1147		1145	β CH
	1126	1099	β CH
1024		1032	β CH
	1015	1004	β CH
981		973	β CH
939		927	β C=O
	928	920	β CC
	888	884	γ CH
848		841	γ CH
	820	813	γ CH
764		766	γ CH
	735	743	γ CH
694		711	γ CC
665		665	γ C=O
625		625	β CN
	560	549	τ CCO
537		537	τ CCO
	511	527	ϕ CN
	501	484	τ CCO
451		455	τ CCO
430	423	427	τ CCN
404	410	408	τ CCH
	388	374	τ CCH

	188	287	τ CCH
-	-	242	τ CCC
-	-	214	τ CCC
-	-	132	τ CCC
-	-	130	τ CCC
-	-	62	τ CCC

ν -stretching; β -in-plane bending; γ -out of plane bending; and τ -torsion.

Table.5

Second order perturbation theory of Fock matrix in NBO basis of 3-Cyano chromone

Donor	Type	Occupancy	Acceptor	Type	Occupancy	E(2)
O 16	n	1.72	C12-C13	π^*	0.21	35.7
O 16	n	1.72	C3-C4	π^*	0.41	25.2
C 1-C2	π	1.68	C3-C4	π^*	0.41	22.2
O 15	n	1.88	C9-12	π^*	0.07	21.9
C 5-C6	π	1.67	C1-C2	π^*	0.29	21.6
C12-C3	π	1.81	C9-O15	π^*	0.23	21.3
C3-C4	π	1.63	C9-O15	π^*	0.23	20.5
O 15	n	1.88	C4-C9	π^*	0.06	19.8
C5-C6	π	1.67	C3-C4	π^*	0.41	18.8
C3-C4	π	1.63	C5-C6	π^*	0.26	18.0
C12-C13	π	1.81	C17-N18	π^*	0.07	17.7
C3-C4	π	1.63	C1-C2	π^*	0.29	16.4
C1-C2	π	1.68	C5-C6	π^*	0.26	16.2
N 18	n	1.97	C12-C17	π^*	0.02	12.4

Table: 6

Theoretical electronic absorption spectra of 3-Cyano chromone (absorption wavelength λ (nm), excitation energies E (eV) and oscillator strengths (f) using TD-DFT/B3LYP/6-311++G(d,p) method.

λ (nm)		E(eV)	(f)	Major contribution
T	E			
Gas				
340		3.642	0.0002	H-1->LUMO (96%)
293		4.231	0.2340	HOMO->LUMO (88%)

282		4.384	0.0725	H-1->L+1 (98%)
254		4.873	0.0019	H-2->LUMO (33%)
252		4.905	0.0052	H-2->LUMO (53%)
239		5.180	0.0226	H-3->LUMO (82%)
236		5.239	0.1153	H-3->L+1 (28%)
232		5.341	0.0043	H-1->L+2 (98%)
228		5.425	0.0006	H-3->L+1 (23%)
226		5.472	0.0021	H-4->LUMO (82%)
Ethanol				
309		4.000	0.0000	H-1->LUMO (95%)
289	270	4.277	0.3116	HOMO->LUMO (91%)
268		4.612	0.0076	H-2->LUMO (43%)
254		4.864	0.0860	H-2->LUMO (48%)
254		4.876	0.0000	H-1->L+1 (97%)
234		5.276	0.1548	H-3->LUMO (82%)
228		5.430	0.1867	H-3->L+1 (16%)
215		5.751	0.0342	H-3->L+1 (50%)
205		6.032	0.0001	H-1->L+2 (98%)
202		6.110	0.0926	H-3->L+1 (11%)

Table.7

Homo - Lumo of 3-Cyano chromone.

Parameters	Gas
E_{HOMO} (eV)	-0.27342
E_{LUMO} (eV)	-0.0247
$\Delta E_{HOMO-LUMO}$ gap (eV)	-0.2095
Electronegativity (χ) (eV)	0.14906
Global hardness (η)(eV)	0.12436
Global softness (S)(eV)	0.49744
Electrophilicity index (ω)(eV)	0.08925
Dipole Moment (μ) (debye)	4.9769

Table 8:

NLO Properties of 3-Cyano chromone

Parameter	a.u.	Parameter	a.u.
α_{xx}	-85.6907	β_{xxx}	157.0949
α_{xy}	8.3911	β_{xyy}	12.6748
α_{yy}	-72.3790	β_{xzz}	-6.9069
α_{xz}	0.0000	β_{yyy}	-21.0180
α_{zz}	-74.9141	β_{yxx}	-16.9895
α_{yz}	-0.0003	β_{yzz}	-0.4301
α_{tot}	-77.6589*	β_{zzz}	-0.0008
	10^{24} esu		
$\Delta\alpha$	190.908*	β_{zyy}	0.0012
	10^{24} esu		

μ_x	6.6090	β_{zxx}	0.0022
μ_y	-3.6704	β_{xyz}	0.0001
μ_z	0.0003	β_{tot}	167.24×10^{-33} esu
μ_{tot}	7.5599		

Table 9:

Thermodynamic properties at different temperatures of 3-Cyano chromone

T (K)	C_m° (cal mol ⁻¹ K ⁻¹)	S_m° (cal mol ⁻¹ K ⁻¹)	ΔH_m° (cal mol ⁻¹ K ⁻¹)
100	13.983	68.576	79.877
200	25.430	83.062	81.834
300	37.314	96.446	84.975

C_m - Heat capacity; S_m -Entropy; ΔH_m -Enthalpy

Table .10

Molecular docking analysis of 3-Cyano chromone

Protein (PDB ID)	Binding energy (kcal/mol)	No. of hydrogen bonds	Bonded Residues	Bond Distance Å
3U3M	5.52	2	PHE 81	3.0
			PRO 90	3.1

ACKNOWLEDGMENTS

We remain grateful to Kanchi Mamunivar Center for Post Graduates studies, Lawspet, Puducherry for providing the Quantum Computational Research Lab for this study.

(A.1)

REFERENCES

[1] Robert Vianelloa, Zvonimir B. Maksica, Tetrahedron 61 (2005) 9381.
 [2] W.D. Watson, in: B.H. Andrew, D. Reidel (Eds.), Interstellar Molecules, Kluwer, Dordrecht, p. 1980.
 [3] J. Benkhoff, Adv. Space Res. 29 (2002) 1177–1186.
 [4] J.P. Ferris, in: S. Patai, Z. Rappaport (Eds.), The Chemistry of Functional Groups, Supplement C, Wiley, Chichester, New York, 1983, p. 325.

[5] Hamdy R. Soltan, Alex. J. Pharm. Sci. 15 (2001) 137.
 [6] Haifeng Song, Kongchang Chen, He. Tian, Dye Pig. 53 (2002) 257.
 [7] Fang Yao, Bin Huang, MingzhongCai, J. Chem. Res. 6 (2009) 366.
 [8] William H. Daly, Munir Arshad, J. Polym. Sci., Polym. Chem. Ed. 22 (1984)975.
 [9] TomizawaMotohiro, Todd T. Talley, David Maltby, Kathleen A. Durkin, KatalinF. Medzihradsky, Alma L. Burlingame, Palmer Taylor, John E. Casida, Proc.Natl. Acad. Sci. USA 104 (2007) 9075.
 [10] S. Cheylan, A. Fraleoni-Morgera, J. Puigdollers, C. Voz, L. Setti, R. Alcubilla, G.Badenes, P. Costa-Bizzarri, M. Lanzi, Thin Solid Films 497 (2006) 16.
 [11] N. Saemian, G. Shirvani, H. Matloubi, J. Radioanal. Nucl. Chem. 268 (2006)545.
 [12] R. Dennington, T. Keith. J. Millam, Gauss view, Semichem Inc., shawnee mission, K. S, 2009, version 9.
 [13] K. Jayasheela, S. Periandy, S. Xavier, K. Niveditha, Docking and spectral investigations (FT-IR, FT-Raman, NMR, UV-Vis) ON 7-Hydroxyl-4-Chromone using quantumComputational (DFT) analysis, [https://doi.org/10.15623/ijret.2018.0702008]
 [14] J. J. Nie, D. J. Xu, Chin. Struct, J. Chem.,21 (2002) 165.
 [15] S. Manohar, R. Nagalakshmi and V. Krishnakumar, SpectrochimicaActa Part A 71 (2008) 110
 [16] G. Mariappan, N. Sundaraganesan, J. Mol. Struct., 1063 (2014) 192.
 [17] J.T. Hoef Surface Science 540 (2003) 441–456
 [18] R.S. Mulliken, J. Chem. Phys. 23 (1955) 1833–1840
 [19] S.K. Wolff, D.J. Grimwood, J.J. Mckinnon, M.J. Turner, D. Jayailaka, M.A. Spackman, University Western, Australia, 2012
 [20] S. Chandra, SpectrochimicaActa Part A 74 (2009) 704-713
 [21] E. K. Sarıkaya, S. Bahçeli, D. Varkal, O. Dereli, Journal of Molecular Structure 1141(2017) 44-52
 [22] V. Karunakaran, V. Balachandran, Spectrochim. Acta A (2014) 1-14
 [23] J.M.Chalmers and P.R.Griffith, Raman Spectroscopy:Theory in Handbook of Vibrational Spectroscopy, Vol. 1 John Wiley & Sons Ltd., New York, (2002) 71–73.
 [24] N.E.H. Belkafouf, F.T. Baara, A. Altomare, R. Rizzi, A. Chouaih, A. Djafri, F. Hamzaoui, Journal of Molecular Structure (2019)
 [25] N. Sundaraganesan, H. Saleem, S. Mohan, M. Ramalingam, V. Sethuraman, Spectrochim. Acta A 62 (2005) 740e751.

- [26] G. Socrates, *Infrared and Raman Characteristic Group Frequencies-Table and charts*, third edition, Wiley, New York, 2001
- [27] J. Arthur, L. Plante, D.H. Stidham, *Spectrochim. Acta A* 74 (2009) 808-818.
- [28] R.N. Singh, A. Kumar, R.K. Tiwari, P. Rawat, *Spectrochim. Acta A* 113 (2013) 378-385
- [29] R. Gayathri, M. Arivazhagan, *Spectrochim. Acta* 97 (2012) 311e325.
- [30] N. Udaya Sri et al., *Molecular and Biomolecular Spectroscopy, SpectrochimActa Part A* 97 (2012) 728-736.
- [31] T. Gnanasambandan, S. Gunasekaran, S. Seshadri, *Spectrochim. Acta* 122(2014) 542e552.
- [32] F. Weinhold, C.R. Landis, *Chem. Educ. Res. Pract.* 2 (2001) 91.
- [33] A. Smith, *Infrared Spectral Interpretation: A Systematic Approach*, CRC Press, Washington, DC, 1999
- [34] K.V. Raman, et al., *Molecular Spectroscopy*, Vijay Nicole Imprints Private Limited, 2004.
- [35] S.I. Gorelsky, *SWizard Program Revision 4.5*, University of Ottawa, Ottawa, Canada, 2010.
- [36] *Journals of computer science and net working* Mekhala. R et al., (2015) *Theoretical science* 2:127 doi[10.4172/2376130X.1000127].
- [37] G. Socrates, *Infrared and Raman Characteristic Frequencies*, 3rd ed., John Wiley & Sons Ltd., Chichester, 2001.
- [38] V.R. Dani, *Organic Spectroscopy*, Tata-Mac Graw Hill Publishing Company, New Delhi, 1995, p. 139.
- [39] T. Koopmans, *Physica* 1 (1934) 104-113.
- [40] R.S. Mulliken, *J. Chem. Phys.* 2 (1934) 782-793.
- [41] R.G. Pearson. *J. Am. Chem. Soc.* 107(1985) 6801-6906.
- [42] W. Yang, P.G. Parr, *Proc. Natl. Acad. Sci. U.S.A.* 82 (1985) 6723-6726.
- [43] P.G. Parr, W. Yang, *Density Functional Theory Of Atoms And Molecules*, Oxford University Press, New York, 1989.
- [44] D.A. Kleinmann, *Phys. Rev.* 126 (1962) 1977-1979.
- [45] E.R. Johndon, S. Keinan, P. Mori-sanchez, J. Conctreas-Garcia, A.J. Cohen, W. Yang, *Revvealing non covalent interactions*, *J. Am. /Chem. Soc.* 132 (18) (2010) 6498-6506.
- [46] W. Humphrey, A. Dalke, K.Schuten, *VMD: Visual molecular dynamics. J. Mol.Graph* 14(1) (1996) 33-38.
- [47] R.F. Bader. *A quatum theory of molecular structure and its applications* *chem. Rev* 91 (5) (1991) 893-928.
- [48] Berger, I., Guttman, C., Amar, D., Zarivach, R., Aharoni, A. *Protein data bank* (2011) *Plos One* 6: e26794-e26794. [10.1371/journal.pone.0026794](https://doi.org/10.1371/journal.pone.0026794)
- [49] K.Jayasheela, Iamya H. Al-wahaibi, S.Periandy, Hanan M. Hassan, S.Sebastian, Xavier, Joseph
- C.Daniel, Ali A. El-Emam, Mohamed I. Attia
Journal of molecular structure 1159 (2018) 83-95